Perturbation theory approach to tunneling: Direct and resonance transmission in super-exchange models

Misha Galperin, Dvira Segal, and Abraham Nitzan
School of Chemistry, Sackler Faculty of Science, Tel Aviv University, Tel Aviv 69978, Israel

(Received 24 September 1998; accepted 31 March 1999)

In this paper we examine, within simple models, different approaches to computing tunneling probabilities in super-exchange models of electron transfer. The relationship between tunneling calculations that use scattering theory type formalisms and approaches based on standing waves, which are more closely related to electron transfer between bound donor and acceptor states, is established. Transmission probabilities computed by using truncated basis representations are compared to exact analytical or numerical results for one- and two-dimensional models. We find that while resonance tunneling is well approximated by truncated basis approaches, computing deep tunneling using such basis sets can lead to large errors. Implications for calculations of bridge assisted electron transfer are discussed. © *1999 American Institute of Physics.*
[S0021-9606(99)01524-X]

I. INTRODUCTION

Recent work on long-range electron transfer has focused on the super-exchange mechanism as the origin of the weak falloff, with distance observed for the transmission probability in many electron transfer systems.[1] The super-exchange mechanism invokes electronic states in the bridge connecting donor and acceptor as intermediate states in the transfer process. The overall transmission probability is then expressed in terms of these states: their energies and the interstate coupling. The transfer parameter β associated with the exponential distance dependence of the transmission probability, $T \sim \exp(-\beta r)$, is obtained in terms of these quantities.[1] Moreover, if these states are energetically close to the donor and acceptor states so that they are actually transiently populated, this distance dependence may become weak or disappear. Also, if thermal relaxation processes erase intermediate coherence, the transmission may take a diffusive character.[2]

The purpose of the present paper is to examine several issues associated with such processes in the absence of thermal relaxation: We develop a steady-state formalism that makes it possible to analyze electron transmission processes in the language of scattering theory, using a representation in which perturbation theory can describe deep tunneling as well as resonance tunneling processes. This also makes it possible to connect scattering theory, which is usually represented in terms of incoming and outgoing waves, with the usual representation of electron transfer theory in terms of initial and final states. We use this formalism within a simple barrier/wells model to show that standard procedures that use truncated basis representations in super-exchange models can fail badly far from resonance. Finally, we discuss the advantages and disadvantages of different computational approaches to the electronic coupling part of the electron transmission problem.

Mathematically, describing the transmission process in super-exchange models in terms of a limited number of bridge states amounts to describing the process in terms of a strongly truncated basis (tight binding approximation). While in the case of resonance tunneling it is expected that near the resonance peak the transmission will be dominated by the states associated with the resonance structure, once we go out of resonance this becomes less obvious. The situation is analogous to that encountered in Raman scattering: Resonance Raman scattering is described well in terms of one or a few intermediate vibronic levels, while the off-resonance process is usually described in terms of the whole intermediate electronic manifold. Intuitively we expect that the energy range of relevant intermediate states is determined by the (inverse of) characteristic time of the transmission process; however, the determination of this time in all but special models is itself uncertain.[3] Related uncertainties arise when we compare transitions between two continua e.g., current through a metal insulator–metal junction, between two discrete levels, e.g., the tunneling splitting in a double-well structure and between a quasibound state and a continuum, e.g., tunneling-induced escape out of a potential well.

The validity of the tight binding approximation for the description of long distance bridge mediated electron transfer was addressed in the past by Beratan *et al.*[4] The model considered below satisfies the criterion $\kappa b \gg 1$ (κ^{-1} is the exponential decay length for the electronic wave function localized on a bridge site and b is the nearest-neighbor distance between such sites) for which, according to Ref. 4, the tight binding approximation should be valid for bridge units that support only one bound state. In contrast, we will show that even though this criterion holds, a truncated basis that uses only the lower states of the bridge sites can lead to substantial errors in the computed transmission for energies far from resonance,[5] in particular when the bridge wells support more than one bound state.

Computing tunneling probabilities is a central issue of quantum transport theory.[6] Recently we have investigated numerically one-electron tunneling processes through water and through rare gas layers,[7] using numerical grid techniques

 © 1999 American Institute of Physics

Downloaded 21 Mar 2004 to 132.66.16.12. Redistribution subject to AIP license or copyright, see http://jcp.aip.org/jcp/copyright.jsp

and a suitable pseudopotential to describe the interaction between the electron and the molecular system. A numerical grid is a basis set chosen so as to accommodate the properties of the one-electron pseudopotential as well as the energy range of interest. In a typical tunneling calculation of this type, we need (in 3D) 100–1000 grid points per atom. If, alternatively, a restricted molecular basis set can be used, a substantial reduction in computational effort may be achieved. For example, recent calculations of electron transmission through conjugated organic molecules[8] use just the four $2s$ and $2p$ atomic orbitals on each carbon atom and one $1s$ orbital on each hydrogen to construct the needed molecular orbitals on the extended Hückel level. (Note that, by construction, such bases are nonorthogonal.) In this context, the question concerning the validity of the tight binding approximation for super-exchange transmission can be rephrased as follows: Assuming that a reliable pseudopotential is available and that a set of local orbitals can also be found, to what extent and under what conditions can a truncated basis of local orbitals describe adequately the transmission process (and therefore be preferred over the spatial grid representation)?

In addition to choosing a convenient basis set to describe the barrier (or, in scattering theory language, the target), we may consider different representations of the initial and final states. Standard descriptions of electron transfer processes compute the rate associated with the decay of population in the initial electronic state that is localized on the donor, or equivalently, the growth of population in the final state localized on the acceptor. The actual process is often dominated by nuclear relaxation about these states, while the bridge levels mediate the electronic coupling. Focusing on the latter issue, the effective donor-acceptor electronic coupling can be estimated from the splitting (or shifts) of the corresponding energy levels from their zero-order values.[1(c),9] Here we adopt the alternative approach of describing the process as a scattering phenomenon. In this description the donor and acceptor states become representatives of the initial and final levels of the scattering continua (that should be summed over when evaluating total transmission probabilities).[8] The resulting observable is relevant for low energy electron transmission (LEET),[10] for photoemission through thin molecular films,[11] for inelastic tunneling spectroscopy (ITS) and scanning tunneling microscopy (STM) through adsorbed molecules,[6] and in measuring the current through molecular spacers between metal contacts.[12] From the theoretical point of view, we deal with the same electronic coupling problem, with the added advantage that the energy is well defined (thus avoiding the difficulty encountered in identifying the exact tunneling energy in electron transfer processes[9]) and can be controlled. One issue, however, requires special attention: For a scattering process, the usual representation in terms of incoming and outgoing waves is natural. On the other hand, the conceptual proximity of electron transmission phenomena to other electron transfer processes suggests that a time-dependent description in terms of semilocal initial and final states, confined to the left and right sides (say) of the barrier, respectively, may be useful. Indeed, we show (Secs. II and III) that scattering theory can be reformulated as a steady-state solution of a time-dependent formalism represented in terms of such semilocal functions. This becomes particularly important when perturbative solutions are sought: The Born approximation in standard scattering theory, as well as any finite-order expansion based on it, cannot describe tunneling. We show in Sec. II that, using a semilocal representation, tunneling through a potential barrier (''through space'' transmission) can be described by perturbation theory in lowest order. Moreover, the description of ''through bond'' transmission and of resonance tunneling (Sec. III) becomes a natural higher order extension of the same calculation, and leads to expressions used by other workers.[8]

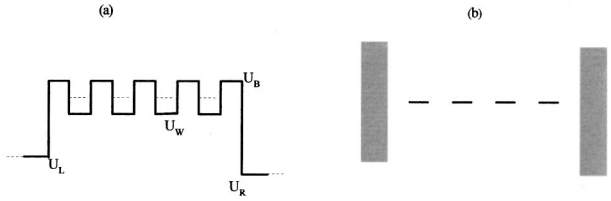

FIG. 1. A simple potential for bridge assisted tunneling processes (a), the corresponding tight binding model (b). Only the lowest states of the intermediate wells are included in the truncated basis shown on the right.

In the present paper we use a simple model of rectangular barriers and wells as a starting point for discussing these issues.[13] In one-dimension, the transmission probability associated with such models can be obtained exactly using transfer matrix methods.[14] On the other hand, the performance of a model that uses, e.g., only the lower bound states of each well as a basis set for the same calculation, can be used as an indication of the validity of similar tight binding approximations used in models for bridge assisted tunneling. Such comparisons are done in Sec. IV, leading to the conclusion that far enough from resonance a strongly truncated basis of the type usually employed [i.e., using the lowest unoccupied molecular orbitals (LUMOs) or the highest occupied molecular orbitals (HOMOs) for electron and hole conduction, respectively] can fail badly in predicting both the magnitude of the electronic coupling, and its dependence on the tunneling length. Similar observations are made also in a model two-dimensional calculation. We conclude (Sec. V) with an assessment of our present ability to compute electron transfer and transmission probabilities using molecular orbitals and pseudopotential methods.

II. PERTURBATION APPROACH TO TUNNELING

Consider the tunneling process associated with the potential barrier displayed in Fig. 1(a). This tunneling process is a one-dimensional scattering problem; however, since the barrier constitutes a strong perturbation in the tunneling regime, it cannot be easily described in low order, e.g., by Born theory. Instead, nonperturbative approaches are usually employed; the most generally used is the Wentzel–Kramers–Brillouin (WKB) approximation. For the rectangular barrier and well structure such as that of Fig. 1(a), an exact solution may be found using the transfer matrix

Downloaded 21 Mar 2004 to 132.66.16.12. Redistribution subject to AIP license or copyright, see http://jcp.aip.org/jcp/copyright.jsp

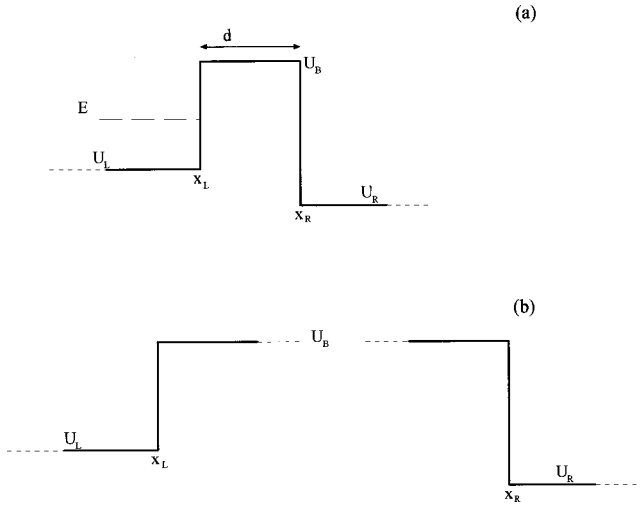

FIG. 2. Tunneling through a simple barrier (a) and the potential used to define the zero-order continuum (standing waves for $E<U_B$ states) (b).

method.[14] Alternatively, it is intuitively expected that a representation in terms of scattering continua plus some states associated with the intermediate wells [Fig. 1(b)] may provide an adequate description of the transmission problem. For electron transfer in a donor-bridge-acceptor system, where the scattering continua are replaced by donor and acceptor states (and supplemented by nuclear relaxation), this is indeed the standard approach.[1,9]

The fact that the transmission probability is very small in many tunneling systems suggests that a perturbation theory of tunneling should be possible using an appropriate representation. Indeed, Bardeen[15] has suggested a perturbation scheme for a simple tunneling barrier (no intermediate wells and no resonance effects) such as that displayed in Fig. 2(a). In the Bardeen formalism the continuum wave unctions are defined as the eigenfunctions of the corresponding half barriers shown in Fig. 2(b), and the transmission probability is expressed in a golden-rule type form where the transition operator is the flux operator defined anywhere within the barrier. The alternative perturbation formalism developed below may be considered a combination of the Bardeen representation of the tunneling problem with the standard quantum chemistry representation of electron transfer. By carrying out this procedure in the framework of an exactly soluble model we will be able to assess the performance of the approximations involved.

Using the potential barrier of Fig. 3(a) as an illustrative example, we first associate the incident and transmitted regions with the half barriers shown in Figs. 3(b) and 3(d), and introduce the corresponding manifold of states,

$$\Psi_l(x;E_l)=\begin{cases} A_l^{(1)}e^{ik_l(x-x_L)}+A_l^{(2)}e^{-ik_l(x-x_L)}; & x<x_0\equiv x_L \\ B_l e^{-\kappa_l(x-x_L)}; & x\geqslant x_0\equiv x_L \end{cases}, \tag{1}$$

$$\Psi_r(x;E_r)=\begin{cases} A_r^{(1)}e^{ik_r(x-x_R)}+A_r^{(2)}e^{-ik_r(x-x_R)}; & x>x_N\equiv x_R \\ B_r e^{\kappa_r(x-x_R)}; & x\leqslant x_N\equiv x_R \end{cases}. \tag{2}$$

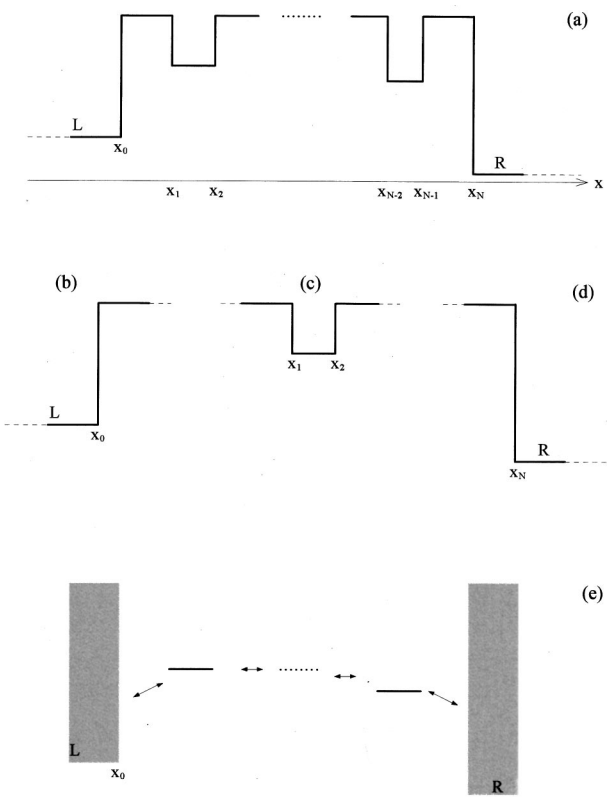

FIG. 3. (a) A potential barrier with intermediate wells. (b), (c), (d) Potentials used to define the zero-order continua and the intermediate zero-order bound states. (e) The energy level diagram for a truncated basis (based on the lowest bound state in each intermediate well) calculation of the transmission rate.

Here, and in what follows, we denote by the subscripts L (or 0) and R (or $N+1$) the incident/reflected region and the transmitted region, respectively, and by the subscript $\alpha\equiv(j,j+1)$ the regions of flat potential defined by $x_j<x\leqslant x_{j+1}$ [see Fig. 3(a)]. Equations (1) and (2) correspond to standing waves with energy E, defined as in the Bardeen formalism using

$$k_l=\frac{1}{\hbar}\sqrt{2m(E_l-U_L)}; \quad \kappa_l=\frac{1}{\hbar}\sqrt{2m(U_{01}-E_l)}, \tag{3}$$

$$k_r=\frac{1}{\hbar}\sqrt{2m(E_r-U_R)}; \quad \kappa_r=\frac{1}{\hbar}\sqrt{2m(U_{N-1,N}-E_r)}.$$

Second, with each intermediate well we associate the set of lower bound states in the corresponding isolated well shown in Fig. 3(c). In the present treatment we limit ourselves to just one (lowest) energy level in each well, e.g., for the well $x_1<x\leqslant x_2$ with the lowest energy state E_{12},

$$\Psi_{12}(x)=\begin{cases} A_{12}^{(1)}e^{ik_{12}x}+A_{12}^{(2)}e^{-ik_{12}x}; & x_1<x\leqslant x_2 \\ B_{12}^{(1)}e^{\kappa_{12}^{(1)}(x-x_1)}; & x\leqslant x_1 \\ B_{12}^{(2)}e^{-\kappa_{12}^{(2)}(x-x_2)}; & x>x_2 \end{cases}, \tag{4}$$

Downloaded 21 Mar 2004 to 132.66.16.12. Redistribution subject to AIP license or copyright, see http://jcp.aip.org/jcp/copyright.jsp

$$k_{12}=\sqrt{\left(\frac{2m}{\hbar^2}\right)(E_{12}-U_{12})};$$

$$\kappa_{12}^{(1)}=\sqrt{\left(\frac{2m}{\hbar^2}\right)(U_{01}-E_{12})}; \tag{5}$$

$$\kappa_{12}^{(2)}=\sqrt{\left(\frac{2m}{\hbar^2}\right)(U_{23}-E_{12})}.$$

Finally, the Hamiltonian $\mathbf{H}_{ij}=\langle\Psi_i|\mathbf{H}|\Psi_j\rangle$ and the overlap $\mathbf{S}_{ij}=\langle\Psi_i|\Psi_j\rangle$ matrix elements are evaluated in terms of the various k and κ parameters and the A and B coefficients (see, e.g., Appendix A). Assuming that the intermediate barriers are high/thick enough, it is possible to disregard these elements for all but nearest-neighbor wells, i.e.,

$$H_{lm}=H_{l1}\delta_{m1};\quad S_{lm}=S_{l1}\delta_{m1},$$

$$H_{rm}=H_{rN_w}\delta_{mN_w};\quad S_{rm}=S_{rN_w}\delta_{mN_w}, \tag{6}$$

$$H_{mm'}=0\quad \text{unless}\quad m'=m\pm 1,$$

where N_w is the number of intermediate wells and $m=1,...N_w$ is the well index. This completes the reduction of the full tunneling problem associated with the multibarrier potential in Fig. 3(a) to the restricted coupled state basis representation of the type displayed in Fig. 3(e). Since nondiagonal coupling and overlap elements are very small when the intermediate barriers are high/thick enough, perturbation theory should work. This is in contrast to the usual scattering theory, which uses free particle states in zero order, where low-order perturbation theory fails for the present problem.

As discussed above, representing the effect of intermediate wells in the barrier by one or a few states per well is equivalent to the standard quantum chemistry approach to electron transfer. Less obvious is the applicability of the continuum states chosen above for calculating direct (''through space'') tunneling by standard perturbation theory. Bardeen's perturbation theory[15] is not easily generalized to the more complex situations discussed below, and we present here an alternative approach. For this purpose we consider the problem of tunneling through a simple rectangular potential barrier [Fig. 2(a). Note that the general notation of Fig. 3 is simplified here by using the notation $x_0\equiv x_L$, $x_1\equiv x_R$, and $U_{01}\equiv U_B$]. The standard calculation of the transmission coefficient for a particle of mass m and energy E incident from the left proceeds by writing the wave function in the form

$$\Psi(x;E)=\begin{cases} A_l^{(1)}e^{ik_lx}+A_l^{(2)}e^{-ik_lx}; & x<x_L \\ A_b^{(1)}e^{\kappa x}+A_b^{(2)}e^{-\kappa x}; & x_L\leqslant x<x_R, \\ A_re^{ik_rx}; & x\geqslant x_R \end{cases} \tag{7}$$

with k_l, k_r, and κ defined by Eq. (3), with E replacing E_l and E_r. The coefficients in Eq. (7) are determined from the four continuity relations for the wave function and its derivatives at the two boundaries. Putting $d=x_R-x_L$ and neglecting terms of order $\exp(-2\kappa d)$ relative to terms of order 1 leads to the following result for the transmission coefficient:

$$\mathbf{T}(E)=\frac{|A_R|^2}{|A_L|^2}\frac{k_R}{k_L}=\frac{16(U_B-E)\sqrt{(E-U_L)(E-U_R)}}{(U_B-U_L)(U_B-U_R)}e^{-2\kappa d}. \tag{8}$$

Consider now the perturbation theory approach to the same problem. Instead of using incoming and outgoing eigenstates of the free particle Hamiltonian, we consider the process as a transition between two interacting continua of the standing waves defined by Eqs. (1) and (2). The couplings and overlaps between these states are given in Appendix A. The transmission problem (from left to right, say) can now be represented as a transition from a particular state, λ, of energy E_λ, from the left ($\{l\}$) manifold, to the continuum manifold of states on the right. Within this subspace of states the operator **H-El** takes the form

$$\begin{pmatrix} E_\lambda & \cdots & H_{\lambda r}-ES_{\lambda r} & \cdots \\ \vdots & \ddots & 0 & 0 \\ H_{r\lambda}-ES_{r\lambda} & 0 & E_r & 0 \\ \vdots & 0 & 0 & \ddots \end{pmatrix}. \tag{9}$$

Note that the submatrix that excludes the first row and column, which corresponds to the $\{r\}$ manifold, is taken diagonally.[16] For the initial value problem with the system in state λ at $t=0$, the transition rate to the right manifold is given by the generalized golden-rule expression (see Appendix B),

$$K_{\lambda\to\{r\}}=2\pi(|H_{\lambda r}-E_\lambda S_{\lambda r}|^2\rho_R)_{E_r=E_\lambda}, \tag{10}$$

where the subscript $E_r=E_\lambda$ indicates, as usual, that all quantities associated with the $\{r\}$ manifold should be computed at energies E_r equal to E_λ.[17] ρ_R is the density of states in the right manifold associated with the spectrum of one-dimensional free particle states. It is given by[18]

$$\rho_R(E_r)=(2\pi|A_R|^2)^{-1}\frac{m}{\hbar^2k_r(E_r-U_r)};$$

$$k_r(E)=[\hbar^{-2}2mE]^{1/2}. \tag{11}$$

Also, the relation between the inverse lifetime of the state λ, $K_{\lambda\to\{r\}}$ of Eq. (10) and the transmission probability $\mathbf{T}(E)$ at energy $E=E_\lambda$, is given by

$$\hbar^{-1}K_{\lambda\to\{r\}}=\mathbf{T}(E_\lambda)\times|A_\lambda|^2\frac{\hbar k_\lambda}{m}. \tag{12}$$

Using the expressions in Appendix A and Eqs. (11) and (12) in Eq. (10) leads again to the result (8). Note that we have limited ourselves to deep tunneling situations by assuming that $e^{-\kappa d}\ll 1$ in the standard tunneling calculation, and by using lowest order in the corresponding perturbation theory approach.

III. BRIDGE ASSISTED TUNNELING AND RESONANCE TUNNELING

Consider now the barriers displayed in Figs. 1 or 3. As discussed above, the transmission through such barriers is an exactly soluble problem. Here we focus on the approximate perturbation theory description of this problem. In this approach, the asymptotic motions to the left and to the right of the barrier are described by standing wave continua as in

Downloaded 21 Mar 2004 to 132.66.16.12. Redistribution subject to AIP license or copyright, see http://jcp.aip.org/jcp/copyright.jsp

Sec. II, while each well is represented by some lower bound states of the corresponding well in Fig. 3(c). For simplicity, we present the following development in the simplest tight binding approximation, using one bound state per well.

Again we note that while we deal with a scattering process, the scattering continua are represented by standing waves that carry no flux. The steady-state formalism used below leads to scattering theory results in this representation. Also, because our representation has nonzero overlap between basis functions, expressions for the transmission cross section will be modified. Similar issues are encountered in the theory of electron transfer when overlapping basis representations are used.[1(c),9]

Denoting the continuous manifolds by $\{l\}$ and $\{r\}$ as before, and the states in the intermediate wells $\{m\}$, with (approximate) energies $E_m=H_{mm}$, $m=1,...N_w$, the solution of the time-dependent Schrödinger equation associated with a particular initial state λ, the incident state in the $\{l\}$ manifold, can be represented by $\Psi(t)=c_\lambda(t)\psi_\lambda+\Sigma_{l\neq\lambda}c_l(t)\psi_l+\Sigma_r c_r(t)\psi_r+\Sigma_m c_m(t)\psi_m$, where the coefficients $c(t)$ satisfy

$$\dot{c}_l+\sum_m S_{lm}\dot{c}_m+\sum_r S_{lr}\dot{c}_r = -iE_lc_l-i\sum_{m=1}^{N_w} H_{lm}c_m-i\sum_r H_{lr}c_r, \tag{13}$$

$$\dot{c}_m+\sum_{(m\neq m')=1}^{N_w} S_{mm'}\dot{c}_{m'}+S_{m\lambda}\dot{c}_\lambda+\sum_{l\neq\lambda} S_{ml}\dot{c}_l+\sum_r S_{mr}\dot{c}_r = -iE_mc_m-i\sum_{(m\neq m')=1}^{N_w} H_{mm'}c_{m'}-iH_{m\lambda}c_\lambda -i\sum_{l\neq\lambda} H_{ml}c_l-i\sum_r H_{mr}c_r;\quad m=1,...N_w, \tag{14}$$

$$\dot{c}_r+\sum_{m=1}^{N_w} S_{rm}\dot{c}_m+S_{r\lambda}\dot{c}_\lambda+\sum_{l\neq\lambda} S_{rl}\dot{c}_l = -iE_rc_r-i\sum_{m=1}^{N_w} H_{rm}c_m-iH_{r\lambda}c_\lambda-i\sum_{l\neq\lambda} H_{rl}c_l. \tag{15}$$

Note that the left and right manifolds were assumed to satisfy $H_{ll'}=E_l\delta_{ll'}$ and $H_{rr'}=E_r\delta_{rr'}$. Note also that while the initial state λ belongs to the $\{l\}$ manifold, we have written it explicitly in Eqs. (14) and (15). Equations (13)–(15) constitute the most general form, where all interstate coupling and overlap terms are included. As already pointed out, when the basis functions $\{m\}$ are spatially localized, a good approximation is often obtained by setting to zero coupling and overlap terms involving centers far enough from each other or from the left and right continua. For large systems this simplification can be numerically significant because it makes the coupling matrix sparse. In addition, the direct coupling between the $\{l\}$ and the $\{r\}$ manifolds will be taken only in the lowest order. This amounts to disregarding the terms $\Sigma_r S_{lr}\dot{c}_r$ and $\Sigma_r H_{lr}c_r$ in Eq. (13) and the terms $\Sigma_{l\neq\lambda}S_{rl}\dot{c}_l$ and $\Sigma_{l\neq\lambda}H_{rl}c_l$ in Eq. (15).

In a time-dependent initial value problem, the set of Eqs. (13)–(15) would be solved for the time-dependent coefficients $c(t)$, given that all coefficients vanish at $t=0$ except $c_\lambda(t=0)=1$. Here we seek a steady-state solution with $|c_\lambda(t)|=1$ at all time. To obtain this solution we repeat the procedure described in the second part of Appendix B, disregarding the time-dependent equation for $c_\lambda(t)$ [one of the equations in the set (13)], and assuming instead that $c_\lambda(t)=c_\lambda e^{-iE_\lambda t}$. In steady state the same holds for all intermediate state amplitudes, i.e., $c_m(t)=c_m e^{-iE_\lambda t}$; $m=1,...N_w$. Using this in Eq. (15) leads to

$$\dot{c}_r=-iE_rc_r-i(H_{r\lambda}-E_\lambda S_{r\lambda})c_\lambda e^{-iE_\lambda t} -i\sum_m (H_{rm}-E_\lambda S_{rm})c_m e^{-iE_\lambda t}, \tag{16}$$

which, following the procedure that leads to Eq. (B11), yields

$$c_r(t)=\left(\tilde{V}_{r\lambda}c_\lambda+\sum_m \tilde{V}_{rm}c_m\right)\frac{e^{-iE_rt}-e^{-iE_\lambda t}}{E_r-E_\lambda} \tag{17}$$

and

$$\frac{1}{|c_\lambda|^2}\frac{d}{dt}\sum_r |c_r(t)|^2=2\pi\left\{\rho_R\left|\tilde{V}_{r\lambda}+\sum_m \tilde{V}_{rm}\frac{c_m}{c_\lambda}\right|^2\right\}_{E_r=E_\lambda}, \tag{18}$$

where the effective coupling $\tilde{V}$ is defined by

$$\tilde{V}_{ab}(E_\lambda)=H_{ab}-E_\lambda S_{ab};\quad a\neq b. \tag{19}$$

Similarly, for $l\neq\lambda$, we get from (13),

$$c_l(t)=\sum_m \tilde{V}_{lm}c_m\frac{e^{-iE_lt}-e^{-iE_\lambda t}}{E_l-E_\lambda}. \tag{20}$$

From (17) and (20) it is evident that only states from $\{r\}$ with $E_r=E_\lambda$ and only states from $\{l\}$ with $E_l=E_\lambda$ are populated significantly, so that we can put $\dot{c}_r(t)=-iE_\lambda c_r$ and $\dot{c}_l(t)=-iE_\lambda c_l$ in the left-hand side (l.h.s) of Eq. (14). This leads to

$$-i(E_\lambda-E_m)c_m=-i\tilde{V}_{m\lambda}c_\lambda-i\sum_{m'\neq m}\tilde{V}_{mm'}c_{m'}-ie^{iE_\lambda t} \times\sum_{l\neq\lambda}\tilde{V}_{ml}c_l(t)-ie^{iE_\lambda t}\sum_r \tilde{V}_{mr}c_r(t). \tag{21}$$

Using Eq. (17), the last term of (21) takes the form

$$-ie^{iE_\lambda t}\sum_r \tilde{V}_{mr}c_r(t) =-i\sum_r \tilde{V}_{mr}\tilde{V}_{r\lambda}\frac{1-e^{i(E_\lambda-E_r)t}}{E_\lambda-E_r}c_\lambda -i\sum_{m'}\left(\sum_r \tilde{V}_{mr}\tilde{V}_{rm'}\frac{1-e^{i(E_\lambda-E_r)t}}{E_\lambda-E_r}c_{m'}\right). \tag{22}$$

Since we are taking the direct coupling between the $\{l\}$ and the $\{r\}$ manifolds only in the lowest order, the first term on the right hand side (r.h.s.) of (22) may be disregarded, and Eq. (22) can be rewritten in the form

Downloaded 21 Mar 2004 to 132.66.16.12. Redistribution subject to AIP license or copyright, see http://jcp.aip.org/jcp/copyright.jsp

$$
\begin{aligned}
&-ie^{iE_\lambda t}\sum_r \tilde{V}_{mr}c_r(t)\\
&\cong -i\sum_{m'}\left(\sum_r \tilde{V}_{mr}\tilde{V}_{rm'}\frac{1-e^{i(E_\lambda-E_r)t}}{E_\lambda-E_r}c_{m'}\right)\\
&=-\sum_{m'}\left(\sum_r \tilde{V}_{mr}\tilde{V}_{rm'}\int_0^t dt e^{i(E_\lambda-E_r)t}c_{m'}\right)\\
&\xrightarrow{t\to\infty} -i\lim_{\varepsilon\to 0}\sum_{m'}\left(\sum_r \frac{\tilde{V}_{mr}\tilde{V}_{rm'}}{E_\lambda-E_r+i\varepsilon}c_{m'}\right)\\
&\equiv -i\sum_{m'}\Lambda^{(R)}_{mm'}c_{m'}, \qquad (23)
\end{aligned}
$$

where the self-energy matrix associated with the right-hand manifold is

$$
\begin{aligned}
\Lambda^{(R)}_{ab}(E_\lambda)&\equiv\lim_{\varepsilon\to 0}\sum_r \frac{\tilde{V}_{ar}\tilde{V}_{rb}}{E_\lambda-E_r+i\varepsilon}\\
&=D^{(R)}_{ab}(E_\lambda)-\frac{1}{2}i\Gamma^{(R)}_{ab}(E_\lambda), \qquad (24)\\
D^{(R)}_{ab}(E_\lambda)&=PP\sum_r \frac{\tilde{V}_{ar}\tilde{V}_{rb}}{E_\lambda-E_r},\\
\Gamma^{(R)}_{ab}(E_\lambda)&=2\pi\sum_r \tilde{V}_{ar}\tilde{V}_{rb}\delta(E_\lambda-E_r), \qquad (25)
\end{aligned}
$$

and where PP denotes principal part of the integral that represents the summation over the continuum. Similarly, from (20),

$$
\begin{aligned}
-ie^{iE_\lambda t}\sum_l \tilde{V}_{ml}c_l(t)&=-i\sum_{m'}\Lambda^{(L)}_{mm'}c_{m'}\\
&=-i\sum_{m'}(D^{(L)}_{mm'}-(1/2)i\Gamma^{(L)}_{mm'})c_{m'}. \qquad (26)
\end{aligned}
$$

Using these results in (21)[19] leads to

$$
c_m=\sum_{m'}[(E_\lambda\mathbf{I}-\tilde{\mathbf{H}}-\Lambda)^{-1}]_{mm'}\tilde{V}_{m'\lambda}c_\lambda;\quad \Lambda=\Lambda^{(L)}+\Lambda^{(R)}, \qquad (27)
$$

where the matrix $\tilde{\mathbf{H}}$ is given by $\tilde{H}_{mm'}=E_m\delta_{mm'}+(V_{mm'}-E_\lambda S_{mm'})(1-\delta_{mm'})$. Inserting Eq. (27) in (18) finally results in

$$
K_{\lambda\to\{r\}}\equiv\frac{1}{|c_\lambda|^2}\frac{d}{dt}\sum_r |c_r(t)|^2=2\pi(\rho_R|T_{r\lambda}|^2)_{E_r=E_\lambda}, \qquad (28)
$$

with $\mathbf{T}=\tilde{\mathbf{V}}+\tilde{\mathbf{V}}\mathbf{G}\tilde{\mathbf{V}}$, and $G_{mm'}=[(E_\lambda\mathbf{I}-\tilde{\mathbf{H}}-\Lambda)^{-1}]_{mm'}$ is evaluated in the $\{m\}$ subspace. In the calculations described below the level shifts $\mathbf{D}$ were disregarded and Λ was replaced by $-i\Gamma$.

Equation (28) is the final result for the steady-state transition rate from an initial level $|\lambda\rangle$ in the $\{l\}$ manifold to the $\{r\}$ manifold. The transition amplitude $\tilde{\mathbf{V}}+\tilde{\mathbf{V}}\mathbf{G}\tilde{\mathbf{V}}$ is seen to be a sum of a direct (or ''through space'') contribution and an indirect component associated with the intermediate states $\{m\}$.[20] The latter term, $\tilde{\mathbf{V}}\mathbf{G}\tilde{\mathbf{V}}$, is most important near resonance, i.e., when the incident energy E_λ is close to an intermediate state energy E_m, but may dominate the transition also in off-resonance situations. The transition rate is determined by contributions from these two routes *as well as from interference between them*. The transmission probability is then found from Eqs. (28) and (12). Note that because all intermediate state couplings are in principle included in the calculation that leads to Eq. (28), this result can be used also for two- and three-dimensional models, e.g., when the ''bridge'' is a molecular layer separating two electrodes.

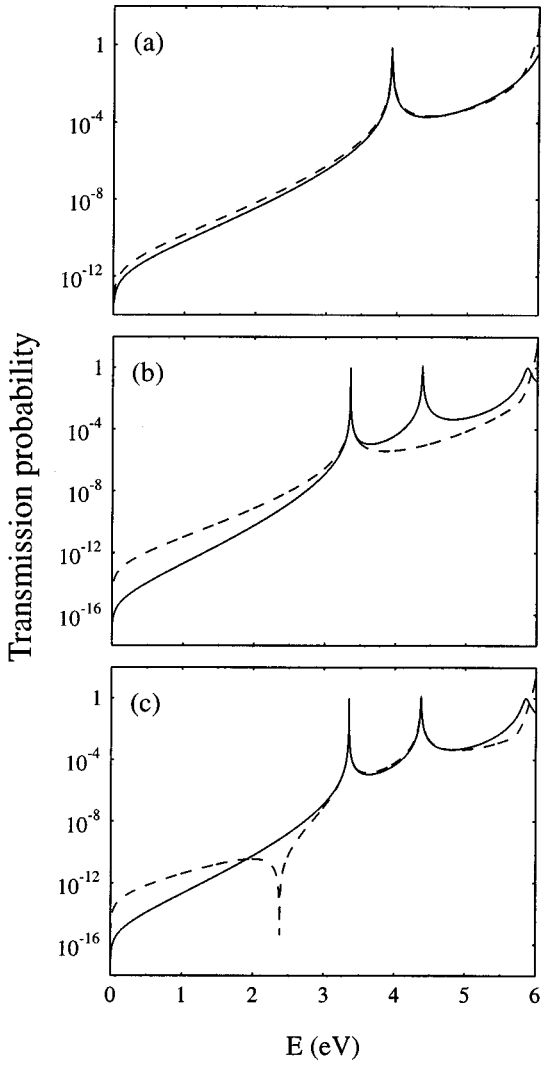

FIG. 4. Transmission probabilities for tunneling through the potential of Fig. 1(a). Full lines—exact results. Dashed lines—results obtained from Eq. (28) using a truncated basis. See text for details of the potential surface and of the truncated basis used.

IV. RESULTS AND DISCUSSION

Figure 4 compares the electron transmission probabilities as functions of the incident energy, obtained from Eqs. (28), to the exact results calculated using the transfer matrix method, for the symmetric model of Fig. 1 with one intermediate well. Here we use $U_B-U_L=U_B-U_R=6$ eV, $U_B-U_W=3$ eV for the barrier height, and $x_1-x_0=x_3-x_2$

Downloaded 21 Mar 2004 to 132.66.16.12. Redistribution subject to AIP license or copyright, see http://jcp.aip.org/jcp/copyright.jsp

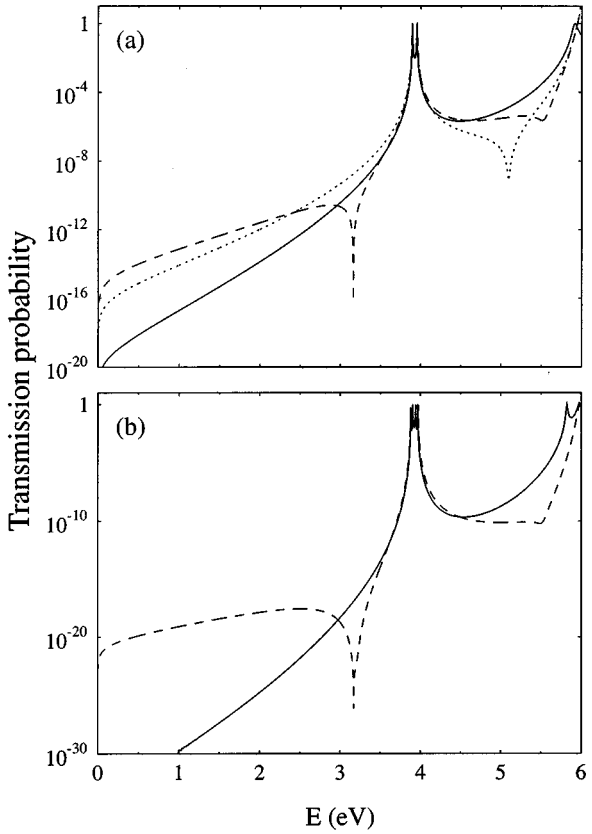

FIG. 5. Results of tunneling calculations for the potential barrier of Fig. 1(a). Full lines—exact results. Dashed lines—results obtained using a truncated basis with the lowest bound state (with the potential parameters used—the only bound state) in each well. Dotted line in Fig. 5(a)—result of the truncated basis approximation with the additional approximation that replaces $\tilde{V}_{12}(E)$ by $\tilde{V}_{12}(E_1)=\tilde{V}_{12}(E_2)$. See text for details of the potential surfaces.

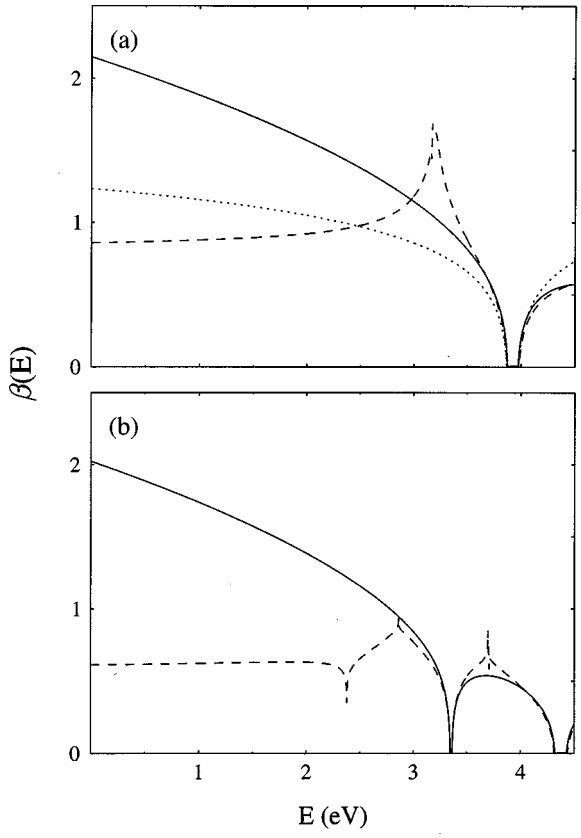

FIG. 6. $\beta(E)$ as a function of the transmission energy E for the model of Fig. 1. See text for details of the potential surfaces and the truncated basis. Line notation is as in Fig. 5.

$=4$ Å for the barrier width parameters. In Fig. 4(a) the intermediate well width was taken $x_2-x_1=4$ Å. This well supports one bound level. Figures 4(b) and 4(c) correspond to an intermediate well width $x_2-x_1=8$ Å, which supports two bound levels. The calculation that leads to Fig. 4(b) uses only the lower of these two intermediate levels in the truncated basis set, while Fig. 4(c) is obtained using both. Figures 5(a) and 5(b) show similar results for two and four intermediate wells, respectively, where all barrier width parameters are taken to be $x_j-x_{j-1}=4$ Å (again supporting one bound level per well).

Figures 6(a) and 6(b) display, as a function of electron energy E, the ''beta parameter,'' $\beta(E)$, which describes the distance dependence of the transition probability according to the ansatz

$$K_{\lambda\to\{r\}}(E_\lambda,d)=A\exp[-\beta(E_\lambda)d], \tag{29}$$

where $d=x_N-x_0$ is the barrier width. β is obtained as the slope of the line describing $\ln(K_{\lambda\to\{r\}}(E_\lambda,d))$ as a function of d. A linear dependence, indicating exponential dependence of K on d, is obtained as long as E_λ is not too close to resonance with the quasibound levels in the intermediate wells. Figure 6(a) corresponds to an extension of the model used in Fig. 4(a). The barrier (Fig. 1) is made of N_w segments of barriers and wells, characterized by equal widths of 4 Å for all intermediate barriers and wells. The barrier used in Figs. 6(b) is an extension of that used in Figs. 4(b) and 4(c), with width parameters equal to 4 Å for all intermediate barriers and 8 Å for all intermediate wells. Thus, the total widths (in Å) of barriers with N_w intermediate wells are $d=4(2N_w+1)$ in the model used in Fig. 6(a) and $d=8N_w+4(N_w+1)$ in the model used in Fig. 6(b), respectively. All the bound states of each well [one in Fig. 6(a), two in Fig. 6(b)] are included in the truncated basis set.

Finally, Fig. 7 shows a simple application of the present formulation for a two-dimensional model: transmission of an incident plane wave traveling in the z direction through the modified two-dimensional rectangular barrier shown in Fig. 7(a). The barrier height is 6 eV and its size in the transmission direction is $d_z=12.4$ Å. In order to conform to the numerical calculation, we also impose periodic boundary conditions in the perpendicular direction x, with a period $d_x=100$ Å. Two identical cylindrical wells of radius 2 Å and depth 3 eV relative to the barrier top are positioned so that their centers are at $(x,z)=(0,-2.2)$ and (0,2.2) Å, respectively, where $z=0$ corresponds to the barrier center. Such a well, in an otherwise constant two-dimensional potential surface, supports one bound state. A numerically exact evaluation of the transmission probability may be obtained using the absorbing boundary conditions Green's function method.[21] The numerical results shown in Fig. 7(b) were obtained using a grid of 200×210 points with spacings $\Delta x=0.5$ and $\Delta z=0.177$ Å and periodic boundary conditions as

Downloaded 21 Mar 2004 to 132.66.16.12. Redistribution subject to AIP license or copyright, see http://jcp.aip.org/jcp/copyright.jsp

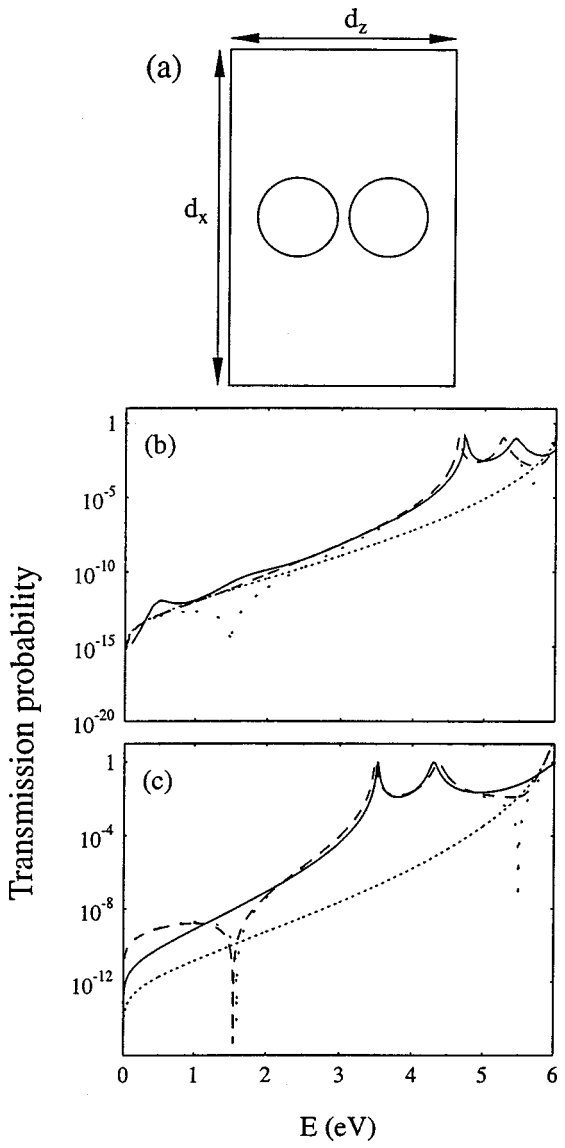

FIG. 7. (a) A sketch of a two-dimensional barrier with two cylindrical wells (see text for details). (b) Transmission probability vs incident energy of a plane wave traveling in the z direction through the two-dimensional barrier shown in Fig. 2(a). Note that periodic boundary conditions are employed in the direction (x) perpendicular to the tunneling. (c) Transmission through the one-dimensional barrier which corresponds to a straight path perpendicular to the tunneling direction connecting the centers of the two wells. Full lines—exact results based on a numerical grid calculation in Fig. 7(b) and on the known analytical result in Fig. 7(c). Dashed lines—results based on the truncated basis approximation using the single bound state in each well. Densely spaced and sparsely spaced dotted lines correspond to the direct and the indirect contributions [Eq. (28)], respectively.

described above. The following absorbing potential was applied at the edges of the z domain: $\varepsilon(z)=0$ for $|z|\leqslant d_z/2$ and $\varepsilon(z)=1.2[(|z|-d_z/2)/(L-d_z/2)]^7$ for $L\geqslant|z|>d_z/2$, where L is half the grid length in the z direction. The resulting transmission probability is compared to a calculation based on a truncated basis set analogous to that used in Fig. 5(a), the left and right continua and the two zero-order bound levels in the wells. The latter calculation uses Eq. (28) in the same way as before, except that two-dimensional wave functions and integrals are used to calculate the needed $\tilde{H}$ and $\tilde{S}$ matrix elements. Figure 7(b) shows the results of the grid calculation, together with those based on the truncated basis approximation. For the latter we show the total transmission probability as well as the independent contributions of the direct ($T=\tilde{V}$) and the indirect ($T=\tilde{V}G\tilde{V}$) components of Eq. (28). Figure 7(c) shows similar results for a one-dimensional barrier obtained by taking a straight path along $z=0$, the line connecting the two well centers. Note that the peaks in Fig. 7(b) lie at higher energies due to the larger value of the two-dimensional zero-point energy.

We note again that in the calculations, which lead to Figs. 4–7, we have disregarded the small energy shifts associated with the real part of Λ [Eq. (24)], i.e., we have neglected the terms D defined in Eq. (25). While this approximation has a very small effect on the quality of the results displayed in Figs. 4–6, its effect is clearly seen in Fig. 7, which corresponds to a system in which narrower barriers, therefore larger couplings, exist between the zero-order well states and the continua.

It is evident from all the results displayed above that tight binding models for bridge assisted tunneling can provide a good description of the transmission process at and not too far from resonance. The quality of this description obviously depends on the number of intermediate quasi-bound barrier states that are included in the truncated basis. Because of the exponential dependence of tunneling on barrier height, one tends to assume that a truncated basis based on the lower energy bridge states should provide a good description for deep tunneling below the resonance regime. This assumption is shown to be wrong. Its failure is seen in Figs. 4–7 in several ways.

(a) Figure 4(a) shows that the deviation of the truncated basis (using the lowest state of each intermediate well) model from the exact result increases as the incident energy decreases below the resonance energy. This deviation increases considerably when the intermediate well supports more than one bound state but only the lowest one is taken in the truncated basis (Fig. 4b). Increasing the basis by taking more zero-order well states may improve the quality of the result at some energies, but may create other problems [see point (b)].

(b) Using truncated bases associated with a finite number of intermediate barrier levels may give rise to interference artifacts that result in unphysical features in the transmission spectrum. This is seen in Fig. 4(c), as well as in Figs. 5(a) and 5(b). With our choice of zero-order basis functions, the dip at $E\cong 2.3$ eV in Fig. 4(c) results from destructive interference between the two pathways associated with the two intermediate levels, while the origin of the unphysical dip at $E\cong 3.2$ eV in Fig. 5 is simply related to the vanishing of the effective coupling $\tilde{V}_{12}=H_{12}-ES_{12}$ between the two intermediate levels at $E=H_{12}/S_{12}$. [It is interesting to note that a cruder approximation which replaces $\tilde{V}_{12}(E)$ by $\tilde{V}_{12}(E_1)$ (here $E_1=E_2$) eliminates this dip, but yields a worse approximation to the exact result in the near resonance region (Fig. 5(a)].

(c) The behavior of the ''β parameter'' as a function of the incident energy E (Fig. 6) shows a dramatic discrep-

Downloaded 21 Mar 2004 to 132.66.16.12. Redistribution subject to AIP license or copyright, see http://jcp.aip.org/jcp/copyright.jsp

ancy between the exact result and the result obtained from the truncated basis representation. The exact dependence of β on the tunneling energy shows a rapid decrease of β when E increases from zero toward the energy of the first resonance. The vanishing of β for resonance transmission indicates that the exponential dependence ansatz, Eq. (29), does not hold at and near the resonance energy, as is well known. The result for $\beta(E)$ using the truncated basis approximation deviates from the exact result in two ways: First, it shows the signature of the unphysical dip in Figs. 5(a) and 5(b) as a maximum in β: As discussed above, this dip is associated with the (unphysical) vanishing of the nearest-neighbor effective coupling $\tilde{V}_{j,j+1}=H_{j,j+1}-ES_{j,j+1}$, which implies a maximum in β at the corresponding energy. Second, at lower incident energies this unphysical β increases rather than decreases with increasing E. This behavior can be traced to the fact that for $|E-E_j|\gg H_{j,j+1}/S_{j,j+1}$ the interstate coupling parameter $|\tilde{V}_{j,j+1}(E)|^2/(E-E_j)$ becomes linear in E_j-E, rather then inversely proportional to it.[22] In the approximation which replaces $\tilde{V}_{j,j+1}(E_\lambda)$ by $\tilde{V}_{j,j+1}(E_j)$ [dotted line in Fig. 6(a)], $\beta(E)$ decreases with increasing E for energies far below resonance, and furthermore the unphysical interference peak is absent. Still, except close to resonance, the value predicted by these approximations strongly deviates from the exact result.

Finally, consider the two-dimensional case of Fig. 7. All considerations discussed in the one-dimensional case apply also here; however, an important additional factor is the fact that the relative contribution of the ''direct'' or ''through space'' route to transmission is now enhanced by the fact that the quasibound intermediate states are localized in relatively small neighborhoods of the barrier. Obviously, for a barrier of infinite spatial size in the direction(s) normal to the tunneling and with a finite number of local intermediate wells, the direct transmission component will always be dominant for an incident plane wave. This is also seen in our model system, characterized by a large finite d_x, by comparing Figs. 7(b) and 7(c). For this reason, the agreement between the exact result and the truncated basis approximation is considerably better in the two-dimensional calculation than in the corresponding one-dimensional system. In the low energy regime, where the indirect tunneling component shows again the unphysical behavior discussed above, the transmission is dominated by the direct component, which, as seen in Sec. III, is described well by our approximation.

In view of the results discussed above it is important to find a criterion for the size of the basis set needed for the calculation of bridge assisted tunneling. This question will be studied separately; however, the following reasoning may be useful: Let $\Delta E=|E-E_B|$ be the energy gap between the tunneling energy E and the nearest bridge level E_B. The bridge level assists tunneling by being virtually occupied on a time scale $\tau=\hbar|E-E_B|^{-1}$. By the same reasoning, other bridge levels B' within the same energy range from E_B, i.e., $|E_{B'}-E_B|\leqslant|E-E_B|$, should be included in the calculation. For the examples described in Sec. IV this will involve continuum states with energies above the barrier top when we go far below resonance.

V. CONCLUSIONS

In this paper we have addressed two issues concerning tunneling transmission across a potential barrier. (1) A relationship was established between the conventional approach that invokes stationary scattering theory and the steady-state solution of the time-dependent theory based on standing wave representation of the incoming and outgoing continua. The latter approximation makes it easier to make contact between the present formalism and between the standard theory of electron transfer between localized donor and acceptor states. (2) For simple super-exchange models we have compared the transmission probability calculated with truncated basis sets to exact analytical or numerical solutions. We have shown that using truncated basis sets based on lower zero-order bound states in the bridge to describe deep tunneling can fail badly, even though such models can describe successfully transmission near the corresponding resonances. We conclude that, for deep tunneling, such calculations should be regarded with caution, and approaches based on appropriate pseudopotentials may sometimes be advantageous.

ACKNOWLEDGMENTS

This research was supported in part by the U.S.A.–Israel Bi-national Science Foundation and by the Israel Ministry of Science. We thank Professor Mark Ratner for many helpful discussions.

APPENDIX A

Here we list, as examples, the expressions for the coupling and overlap matrix elements between the wave functions defined in Eqs. (1) and (2). We focus on the simple barrier case described by Fig. 2, for which the different k's and κ's are given by Eq. (3) with $U_{01}=U_{N-1,N}=U_B$. Continuity conditions yield

$$A_l^{(2)}=-\frac{\kappa_l+ik_l}{\kappa_l-ik_l}A_l^{(1)};\quad B_l=-\frac{2ik_l}{\kappa_l-ik_l}A_l^{(1)}, \tag{A1}$$

and, similarly,

$$A_r^{(2)}=-\frac{\kappa_r-ik_r}{\kappa_r+ik_r}A_r^{(1)};\quad B_r=\frac{2ik_r}{\kappa_r+ik_r}A_r^{(1)}. \tag{A2}$$

It is convenient to express the overlap matrix elements between ''right'' and ''left'' states as a sum over contributions from regions L ($x<x_L$), B ($x_L\leqslant x<x_R$), and R ($x\geqslant x_R$): see Fig. 2,

$$S_{lr}\equiv\int_{-\infty}^{\infty}dx\Psi_l^*(x)\Psi_r(x)=\mathbf{S}_{lr}^L+\mathbf{S}_{lr}^B+\mathbf{S}_{lr}^R, \tag{A3}$$

where $\mathbf{S}_{lr}^L\equiv\int_{-\infty}^{x_L}dx\Psi_l^*(x)\Psi_r(x)$, $\mathbf{S}_{lr}^B\equiv\int_{x_L}^{x_R}dx\Psi_l^*(x)\Psi_r(x)$, and $\mathbf{S}_{lr}^R\equiv\int_{x_R}^{\infty}dx\Psi_l^*(x)\Psi_r(x)$ are given by

$$S_{lr}^L=-4A_L^{(1)*}A_R^{(1)}\frac{k_lk_r(\kappa_l+\kappa_r)}{(\kappa_l+ik_l)(\kappa_r+ik_r)(k_l^2+\kappa_r^2)}e^{-\kappa_r d}, \tag{A4}$$

Downloaded 21 Mar 2004 to 132.66.16.12. Redistribution subject to AIP license or copyright, see http://jcp.aip.org/jcp/copyright.jsp

$$S_{lr}^{R}=-4A_{L}^{(1)*}A_{R}^{(1)}\frac{k_l k_r(\kappa_l+\kappa_r)}{(\kappa_l+ik_l)(\kappa_r+ik_r)(k_r^2+\kappa_l^2)}e^{-\kappa_l d}, \quad \text{(A5)}$$

$$S_{lr}^{B}=4A_{L}^{(1)*}A_{R}^{(1)}\frac{k_l k_r}{(\kappa_l+ik_l)(\kappa_r+ik_r)}\frac{e^{-\kappa_l d}-e^{-\kappa_r d}}{\kappa_l-\kappa_r}. \quad \text{(A6)}$$

In terms of these partial overlaps the Hamiltonian matrix elements between states from the $\{l\}$ and $\{r\}$ manifolds are easily shown to be given by

$$\mathbf{H}_{lr}\equiv\int_{-\infty}^{\infty}dx\Psi_l^*(x)\mathbf{H}\Psi_r(x)$$
$$=E_r\mathbf{S}_{lr}-(U_B-U_L)\mathbf{S}_{lr}^{L}=E_l\mathbf{S}_{lr}-(U_B-U_R)\mathbf{S}_{lr}^{R}. \quad \text{(A7)}$$

APPENDIX B

Here we derive the generalized golden rule given by Eq. (10). It should be noted that this generalization corresponds to a situation where nonzero overlap exists between initial and final states, and some care has to be exercised in its derivation under this circumstance. To this end, analyze the decay of an initial level coupled to a continuum of states in a representation defined by Eq. (9). It will prove useful to consider both the initial value problem and the steady-state solution.

1. The initial value problem

Let the time-dependent wave function be of the form

$$\Psi(t)=c_l(t)\psi_l+\sum_r c_r(t)\psi_r, \quad \text{(B1)}$$

with $c_l(t=0)=1$ and $c_r(t=0)=0$. Inserting (B1) into the time-dependent Schrödinger equation leads to equations for the coefficients c,

$$\dot{c}_l+\sum_r S_{lr}\dot{c}_r=-iE_l c_l-i\sum_r H_{lr}c_r,$$
$$S_{rl}\dot{c}_l+\dot{c}_r=-iH_{rl}c_l-iE_r c_r. \quad \text{(B2)}$$

Solving by Laplace transform, $\hat{c}(z)=\int_0^\infty dte^{-zt}c(t)$, we get

$$\hat{c}_l(z)=\left(1-\sum_r\frac{(zS_{lr}+iH_{lr})S_{rl}}{z+iE_r}\right)\times\left[z+iE_l-\sum_r\frac{(zS_{lr}+iH_{lr})(zS_{rl}+iH_{rl})}{z+iE_r}\right]^{-1}. \quad \text{(B3)}$$

Note that if all the overlap terms S vanish, Eq. (B3) is reduced to

$$\hat{c}_l(z)=\left[z+iE_l+\sum_r\frac{|H_{lr}|^2}{z+iE_r}\right]^{-1}, \quad \text{(B3}')$$

which, upon employing inverse Laplace transform and after standard transformations, yields $c(t)$ in the form

$$c_l(t)=\frac{1}{2\pi}\int_{-\infty}^{\infty}dEe^{-iEt}\frac{1}{E-E_l-\Lambda_{ll}(E+i\eta)}, \quad \text{(B4)}$$

where

$$\Lambda_{ll}(z)=\sum_r\frac{|H_{lr}|^2}{z-E_r} \quad \text{(B5)}$$

and $\eta\to 0$. If the energy dependence of Λ_{ll} can be disregarded near $E\cong E_l$, Eq. (B4) leads to $c_l(t)=e^{-i\tilde{E}_l t-(\Gamma_l/2)t}$, with $\tilde{E}_l=PP\Sigma_r|H_{lr}|^2/(E_l-E_r)$ and

$$\Gamma_l=K_{l\to\{r\}}=2\pi\sum_r|H_{lr}|^2\delta(E_l-E_r)=2\pi(|H_{lr}|^2\rho_R)_{E_r=E_l}. \quad \text{(B6)}$$

To extract similar information from Eq. (B3) we disregard the correction to unity in the numerator, and rewrite the rest of the expression for $\hat{c}_l(z)$ in the form[23]

$$\hat{c}_l(z)=\frac{1}{z+iE_l+\sum_r\frac{|H_{lr}-izS_{lr}|^2}{z+iE_r}}. \quad \text{(B7)}$$

The same procedure used to get Eqs. (B4) and (B5) from Eq. (B3′) now leads again to Eq. (B4), with Eq. (B5) replaced by

$$\Sigma_{ll}(z)=\sum_r\frac{|H_{lr}-zS_{lr}|^2}{z-E_r}. \quad \text{(B8)}$$

Obviously, the golden-rule expression (B6) now becomes

$$\Gamma_l=2\pi(|H_{lr}-E_lS_{lr}|^2\rho_R)_{E_r=E_l}, \quad \text{(B9)}$$

as claimed.

2. Steady-state solution

Starting again from Eq. (B2), we now consider a steady state in which the amplitude of the level l is restricted, by some unspecified means, to behave as if the level was not coupled to the $\{r\}$ continuum, i.e., $c_l(t)=c_l e^{-iE_l t}$, where the constant c_l can be chosen to be 1. We want to compute the steady-state rate of transferring population to the continuum. Using the lower of Eqs. (B2) in the form

$$\dot{c}_r=-iE_r c_r-i(H_{rl}-E_lS_{rl})e^{-iE_l t}c_l, \quad \text{(B10)}$$

yields

$$c_r(t)=(H_{rl}-E_lS_{rl})\frac{e^{-iE_r t}-e^{-iE_l t}}{E_r-E_l}c_l \quad \text{(B11)}$$

and

$$\sum_r|c_r(t)|^2=4|c_l|^2\int dE_r\rho(E_r)|H_{lr}-E_lS_{rl}|^2\times\frac{\sin^2[\frac{1}{2}(E_l-E_r)t]}{(E_l-E_r)^2}. \quad \text{(B12)}$$

For $t\to\infty$, $\sin^2(xt/2)/x^2\to 1/2\pi t\delta(x)$, so

$$K_{l\to\{r\}}\equiv\frac{1}{|c_l|^2}\frac{d}{dt}\sum_l|c_r(t)|^2=2\pi(|H_{lr}-E_lS_{lr}|^2\rho_R)_{E_r=E_l}. \quad \text{(B13)}$$

Downloaded 21 Mar 2004 to 132.66.16.12. Redistribution subject to AIP license or copyright, see http://jcp.aip.org/jcp/copyright.jsp

[1] (a) H. M. McConnell, J. Chem. Phys. **35**, 508 (1961); (b) S. Larsson, J. Am. Chem. Soc. **35**, 508 (1981); M. A. Ratner, J. Phys. Chem. **94**, 4877 (1990); (c) M. D. Newton, Chem. Rev. **91**, 767 (1991), and references therein.

[2] W. T. Pollard, A. K. Felts, and R. A. Friesner, Adv. Chem. Phys. **93**, 77 (1996); A. K. Felts, W. T. Pollard, and R. A. Friesner, J. Phys. Chem. **99**, 2929 (1995); E. S. Medvedev, and A. A. Stuchebrukhov, J. Chem. Phys. **107**, 3821 (1997); A. Okada, V. Chemyak, and S. Mukamel, J. Phys. Chem. A **102**, 1241 (1998); S. S. Skourtis, and S. Mukamel, Chem. Phys. **197**, 367 (1995); B. W. Davis, M. R. Wasielewski, M. A. Ratner, V. Mujica, and A. Nitzan, J. Phys. Chem. A **101**, 6158 (1997).

[3] M. Buttiker and R. Landauer, Phys. Rev. Lett. **49**, 1739 (1982); Phys. Scr. **32**, 429 (1985); E. H. Hauge and J. A. Stovneng, Rev. Mod. Phys. **61**, 917 (1989), and references therein.

[4] D. N. Beratan, J. N. Onuchic, and J. J. Hopfield, J. Chem. Phys. **83**, 5325 (1985).

[5] The numerical results in Ref. 4 also indicate that the proximity to resonance is a factor that determines the accuracy of the tight binding approximation.

[6] See, e.g., E. Wolf, *Principles of Electron Tunneling Spectroscopy* (Oxford University Press, New York, 1985); H. Grabert and H. Michel, in NATO ASI Ser. Ser. B **294** (1988); Chunli Bai, *Scanning Tunneling Microscopy and Its Application*, Springer Series in Surface Sciences, No. 32 (Springer Verlag, Berlin, 1995).

[7] A. Mosyak, A. Nitzan, and R. Kosloff, J. Chem. Phys. **104**, 1549 (1996); A. Mosyak, P. Graf, I. Benjamin, and A. Nitzan, J. Phys. Chem. A **101**, 429 (1997); I. Benjamin, D. Evans, and A. Nitzan, J. Phys. Chem. **106**, 6647 (1997); J. Chem. Phys. **106**, 1291 (1997); A. Haran, K. Kadyshevitch, H. Cohenn, R. Naaman, D. Evans, T. Seidman, and A. Nitzan, Chem. Phys. Lett. **268**, 475 (1977).

[8] See, e.g., C. Joachim, J. K. Gimzewski, R. R. Schlitter, and C. Chavy, Phys. Rev. Lett. **74**, 2102 (1995), and references therein; V. Mujica, M. Kemp, and M. A. Ratner, J. Chem. Phys. **101**, 6849 (1994); **101**, 6856 (1994); M. B. Samanta, W. Tian, S. Datta, J. I. Henderson, and C. P. Kubiak, Phys. Rev. B **53**, 7626 (1996).

[9] S. S. Skourtis and J. N. Onuchic, Chem. Phys. Lett. **209**, 171 (1993); S. Priyadarshy, S. S. Skourtis, S. M. Risser, and D. N. Beratan, J. Chem. Phys. **104**, 9473 (1996); A. A. Stuchebrukhov, Chem. Phys. Lett. **265**, 643 (1997).

[10] L. Sanche, Scanning Microsc. **9**, 619 (1995).

[11] R. Naaman, R. Haran, A. Nitzan, D. Evans, and M. Galperin, J. Phys. Chem. B **102**, 3658 (1998).

[12] See C. Joachim, J. K. Gimzewski, R. R. Schlitter, and C. Chavy, Phys. Rev. Lett. **74**, 2102 (1995), and references therein; V. Mujica, M. Kemp, and M. A. Ratner, J. Chem. Phys. **101**, 6849 (1994), and references therein; **101**, 6856 (1994); M. P. Samanta, W. Tian, S. Datta, J. I. Henderson, and C. P. Kubiak, Phys. Rev. B **53**, 7626 (1996), and references therein.

[13] A limiting case of this model was used before for analyzing bridge mediated electron transfer in Ref. 4.

[14] See, e.g., J. S. Walker and J. Gathright, Comput. Phys. **6**, 393 (1992).

[15] J. Bardeen, Phys. Rev. Lett. **6**, 67 (1961).

[16] In fact, matrix elements $H_{ll'}$ and $H_{rr'}$ between states of the same manifolds are nonzero but much smaller than those that mix states from the different manifolds, and are disregarded.

[17] The coupling $H_{\lambda r}-E_{\lambda}S_{\lambda r}$ appearing in this result could be deduced from the energy splitting between two states, degenerate in zero order. $\Delta E=(H_{\lambda r}-E_{\lambda}S_{\lambda r})/(1-|S_{\lambda r}|^2)$ see A. A. Stuchehrukhor, Chem. Phys. Lett. **265**, 643 (1997). The correction to unity in the denominator can be disregarded under our model assumptions.

[18] Taking $|A_R|^2=L^{-1}$, where L is the normalization volume, the factor $(2\pi|A_R|^2)^{-1}=L/2\pi$ is recognized as the density of momentum states in one dimension.

[19] At this point we approximate $\Sigma_{l\neq\lambda}$ by Σ_l.

[20] The association of the $\tilde{V}$ and $\tilde{\mathbf{V}}\mathbf{G}\tilde{\mathbf{V}}$ terms with ''direct'' and ''indirect'' contributions is to a large extent a matter of definition. In off-resonance situations, where the intermediate manifold $\{m\}$ is not populated, also the second term could be viewed as direct.

[21] T. Seidman and W. H. Miller, J. Chem. Phys. **96**, 4412 (1992); **97**, 2499 (1992). For applications to tunneling, see A. Mosyak, A. Nitzan, and R. Kosloff, J. Chem. Phys. **104**, 1549 (1996); A. Mosyak, P. Graf, I. Benjamin, and A. Nitzan, J. Phys. Chem. A **101**, 429 (1997); I. Benjamin, D. Evans, and A. Nitzan, J. Phys. Chem. A **106**, 6647 (1997); J. Chem. Phys. **106**, 1291 (1997); A. Haran, K. Kadyshevitch, H. Cohenn, R. Naaman, D. Evans, T. Seidman, and A. Nitzan, Chem. Phys. Lett. **268**, 475 (1977).

[22] $H_{j,j+1}$ can be estimated by $(H_{jj}+H_{j+1,j+1})S_{ij}\cong E_jS_{ij}$. Therefore V_{ij} depends approximately linearly on $|E_i-E_{\lambda}|$.

[23] Note that we anticipate here that z is purely imaginary.

Downloaded 21 Mar 2004 to 132.66.16.12. Redistribution subject to AIP license or copyright, see http://jcp.aip.org/jcp/copyright.jsp